The 58,60Ni (d,n) 59,61Cu Reactions at 25 MeV

I. 4. The ^{58,60}Ni (d,n) ^{59,61}Cu Reactions at 25 MeV

*Inomata T ,Tohei T., Nakagawa T., Terakawa A., Narita A., Matsumoto T., Orihara H. *, Ishii K. *, Hosaka M. *, Miyamoto S. *, Guan Z. *, Ishimaru Y. * Miura K**. and Ohnuma H.****

Department of Physics, Tohoku University
*Cyclotron and Radioisotope Center, Tohoku University**
*Tohoku Institute of Technology***
*Department of Physics, Tokyo Institute of Technology****

Single-particle transfer reactions are well used for the spectroscopic study of single-particle (hole) states of the nucleus. Those reactions are very important to obtain the spectroscopic factors for the states of residual nuclei and the ground state configuration of target nuclei.

The (d,n) reaction at higher incident energy is preferable to get more precise spectroscopic information for single proton states, at present.

Until now many (d,n) reactions have been studied using the deuteron beam of the incident energy 25 MeV accelerated by the AVF cyclotron in Cyclotron and Radioisotope Center Tohoku University (CYRIC). At this incident energy the direct reaction process is considered to take place mainly. As a result, we have got reasonable results of spectroscopic factors for p & sd-shell nuclei.

This time, based on above systematic results, we extend the (d,n) reaction at 25 MeV for the Ni-isotopes under the same consideration. The Z=28 Ni-isotopes have the $1f_{7/2}$ proton closed-shell in a simple shell-model. However, as observed also in our experiment, it is reported that there exist about 10 % hole probabilities of the shell-model limit for the $1f_{7/2}$ orbit.

The experiment was accomplished at CYRIC using 44 m TOF facility[1,2]. Targets consisted of self-supporting foils with 8.1 and 7.1 mg / cm^2 thicknesses for ^{58}Ni and ^{60}Ni, respectively. They were isotopically enriched to 99.9%. Angular distributions were measured at laboratory angles between 10° and 60° with steps of 3° or 5° using a beam swinger system.

In the excitation range up to 10 MeV, many states with the ℓ=1 4 transfer momenta have been observed for ^{59,61}Cu. The energy resolution for large peaks near the ground states was about 200 keV FWHM in both reactions (Fig. 1). Angular distributions of the cross sections were analyzed with distorted wave Born approximation (DWBA) using the code DWUCK4[3,4]. Finite range and nonlocality corrections were applied to these calculations and

the method of Vincent & Fortune[5] was carried out to analyze unbound states. To consider the effect on deuteron break up, the adiabatic approximation by Johnson & Soper[6] was used in the incident channel. In this approximation optical model potentials of Becchetti & Greenless[7] and Carlson et al. [8] were used for protons and neutrons respectively. The potential parameters of Carlson et al. were also used for the neutron of the outgoing channel. Differential cross sections for about 30 peaks in the ^{58}Ni (d,n) ^{59}Cu reaction and 20 peaks in the ^{60}Ni (d,n) ^{61}Cu reaction were analyzed with this treatment. In many cases, these angular distributions have been well reproduced with the present analyses for the various orbital angular momenta ℓ=1, 2, 3 and 4 as shown in Fig. 2, typically.

The sum rules for the shell model orbits can be used to determine the number of the holes for each ℓ in the target nuclei. Figure 3 shows the results of the sum for the spectroscopic factors of each ℓ. In the figure the dotted lines show the shell-model limits and the solid lines show the obtained amounts in the present work. The ℓ=1 and 3 states are considered to distribute at comparatively lower excitation energies in a simple shell-model prediction. In fact, large fractions of the strength for these transfers have been observed in ^{61}Cu. On the other hand, the strengths for the ℓ=3 transfer have been almost fully observed but ones for the ℓ=1 transfer not enough in ^{59}Cu. One of the interesting subjects in this study is to get the information for the hole strengths of $1f_{7/2}$ Dependence of the sum of the present spectroscopic factors on neutron number is consistent with both (^{3}He,d)[9] and (d,^{3}He)[10,11,12,13] results (Fig. 4). But the absolute magnitude of the sum in this experiment are about 60 % of those of the (^{3}He,d) experiments[10,11]

The present experimental spectroscopic factors are compared with these of the (^{3}He,d) experiments (Table 1, 2). There are some differences between our results and the (^{3}He,d) ones for some states even in lower excitation region.

Single-particle energies for shell model orbits and relative occupation probabilities of each orbit for the ground states in both nuclei were derived using our results and those of the (d,^{3}He) reaction[10,11]. Then, Fermi energies were obtained by fitting to these results with the BCS function (Fig. 5). As shown in the figure, single particle energies for each orbit and Fermi energies decrease with neutron number. These mass dependences agree with the recent report[11]

In conclusion, we have observed many proton single particle states in ^{59,61}Cu by the (d,n) reaction at 25 MeV in the excitation energy region up to 10 MeV and got the spectroscopic factors for these states. The adiabatic approximation for the deuteron channel has been successfully applied to explain the angular distributions of emitted neutrons. The $1f_{7/2}$ hole-strengths were derived and the occupation probabilities of the ground states were obtained Using our results and the pick-up results on the same targets.

References

1) Orihara H. and Murakami T.. Nucl. Instrum. and Meth. **188** (1981) 15.
2) Orihara H. et al., Nucl. Instrum. and Meth. **A257** (1987) 189.
3) Kunz P. D. A distorted-wave born approximation code. Univ. Colorado, unpublished.
4) Comfort J. R., Extended version for the program. unpublished.
5) Vincent C. M.. and Fortune H. T., Phys. Rev. **C2** (1970) 782.
6) Johnson R. C. and Soper P. J. R., Phys. Rev. **C 1** (1970) 976.
7) Becchetti F. D. and Greenlees G. W., Phys. Rev. **182** (1969) 1190.
8) Carlson J. D. et al., Nucl. Phys. **A249** (1979) 15.
9) Britton R. M. and Watson D. L., Nucl. Phys. **A272** (1976) 91.
10) Seeger M. et al., Nucl. Phys. **A533** (1991)1.
11) Reiner K. et al., Nucl. Phys. **A472** (1987) 1.
12) Mairle G. et al., Nucl. Phys. **A543** (1992) 558.
13) Marinov A. et al., Nucl. Phys. **A431** (1984) 317.
14) Nucl. Data Sheets. **38** (1983) 4.
15) Gupta H. M. Sen, et al., Nucl. Phys. **A512** (1990) 97.

Table 1. Experimenal spectroscopic strengths in ^{59}Cu

Table 1. Experimental spectroscopic strengths in ^{59}Cu

	^{58}Ni(d,n)^{59}Cu present			^{58}Ni(^{3}He,d)^{59}Cu [14]			
#	E_x	nℓj	$(2j+1)C^2S$	E_x	ℓ	j	$(2j+1)C^2S$
1	0.00	$2p_{3/2}$	1.43	0.000	1	$3/2^-$	1.95
2	0.49	$2p_{1/2}$	0.63	0.491	1	$1/2^-$	0.80
3	0.91	$1f_{5/2}$	2.42	0.912	3	$5/2^-$	4.42
4	1.40	$1f_{7/2}$	0.28	1.400	3	$7/2^-$	0.41
5	1.85	$1f_{7/2}$	0.06	1.865	3	$7/2^-$	–
6	2.32	$2p_{3/2}$	0.18	2.321	1	$3/2^-$	0.24
7	2.71	$1f_{7/2}$	0.06	2.713	3	$7/2^-$	0.16
8	3.04	$1g_{9/2}$	2.33	3.043	4	$9/2^+$	4.41
	3.10	$2p_{1/2}$	0.25	3.124	1	$1/2^-$	0.32
9	3.58	$2d_{5/2}$	0.52	3.581	2	$5/2^+$	0.78
				3.619	1	$1/2^-$	0.14
10	3.94	$2p_{3/2}$	**0.84**	3.904	1	$1/2^-$	0.41
		$2p_{1/2}$	0.88				
11	4.32	$1f_{5/2}$	1.76	4.300	3	$5/2^-$	1.80
	4.35	$2p_{1/2}$	0.11	4.349	1	$1/2^-$	0.44
12	4.81	$2p_{3/2}$	0.11	4.830	1		0.17
		$1g_{9/2}$	0.09	4.939	4		0.05
13	5.27	$2p_{1/2}$	0.13	5.238	1		0.21
14	5.63	$1f_{5/2}$	0.17	5.665	4		0.22
15	5.90	$1g_{9/2}$	0.39	5.950	4		0.27
16	6.24	$1g_{9/2}$	0.65	6.201	4		0.91
17	6.54	$1g_{9/2}$	0.35	6.632	4		0.10
18	6.90	$1g_{9/2}$	1.73	6.847	4		1.00
				6.916	4		1.70
19	7.18	$2d_{5/2}$	0.15	7.116	2		0.21
		$1g_{9/2}$	0.23				
20	7.45	$1g_{9/2}$	0.33	7.396	2		0.23
		$1f_{5/2}$	0.16	7.489	(4)		
21	7.73	$1g_{9/2}$	0.43	7.692	4		0.22
		$2d_{5/2}$	0.09	7.725	2		0.04
22	7.94	$1g_{9/2}$	0.32	7.904	4		0.17
		$2d_{5/2}$	0.01	7.948	2		0.09

Table. 1. continued

23	8.23	$1g_{9/2}$	0.50	8.256	2	0.23
		$2d_{5/2}$	0.21			
24	8.63	$1g_{9/2}$	0.42	8.550	4	0.22
25	9.06	$1g_{9/2}$	0.15			
		$2d_{5/2}$	0.04			
26	9.28	$1g_{9/2}$	0.32			
		$2d_{5/2}$	0.07			
27	9.78	$1g_{9/2}$	0.10			
		$2d_{5/2}$	0.07			
28	10.13	$1g_{9/2}$	0.10			
		$2d_{5/2}$	0.08			
29	10.50	$1g_{9/2}$	0.12			
		$2d_{5/2}$	0.08			

Table. 2. Experimental spectroscopic strengths in ^{61}Cu.

	^{60}Ni(d,n)^{61}Cu present			^{60}Ni(^{3}He,d)^{61}Cu [15]		
#	E_x	nℓj	$(2j+1)C^2S$	E_x	$n\ell j$	$(2j+1)C^2S$
1	0.00	$2p_{3/2}$	2.10	0.000	2p3/2	1.79
2	0.49	$2p_{1/2}$	1.04	0.477	2p1/2	0.91
3	0.99	$1f_{5/2}$	2.79	0.972	1f5/2	3.26
4	1.33	$1f_{7/2}$	0.33	1.310	1f5/2	0.49
		$1f_{5/2}$	0.32	1.394	1f7/2	0.47
5	1.97	$2p_{3/2}$	0.28	1.933	2p3/2	0.40
6	2.13	$\{$ $1f_{5/2}$	**0.40**	2.107	2p1/2	0.11
		$\{$ $\mathbf{2p_{1/2}}$	**0.03**	2.220	1f5/2	0.71
		$\{$ $1f_{5/2}$	0.39			
		$\{$ $2p_{3/2}$	0.03			
7	2.36	$\{$ $1f_{7/2}$	0.15			
		$\{$ $2p_{1/2}$	0.08			
		$\{$ $\mathbf{1f_{7/2}}$	**0.14**	2.399	1f7/2	
		$\{$ $\mathbf{2p_{3/2}}$	**0.08**			
8	2.85	$\{$ $1g_{9/2}$	2.29	2.720	1g9/2	3.77
		$\{$ $2p_{3/2}$	0.24	2.851	2p1/2	0.32
		$\{$ $\mathbf{1g_{9/2}}$	2.32			
		$\{$ $\mathbf{2p_{1/2}}$	0.24			
9	3.06	$2p_{3/2}$	0.32	3.078	2p1/2	0.33
		$\mathbf{2p_{1/2}}$	**0.33**			
10	3.44	$2d_{5/2}$	0.56	3.426	2d5/2	0.59
11	3.86	$\{$ $\mathbf{2d_{5/2}}$	**0.06**	3.601	2d5/2	0.20
		$\{$ $\mathbf{2p_{1/2}}$	**0.09**	3.863	2p1/2	0.13
		$\{$ $2d_{5/2}$	0.05			
		$\{$ $2p_{3/2}$	0.10			
12	4.49	$1f_{5/2}$	0.20	4.484	1f5/2	0.45
		$1f_{5/2}$	0.35			
13	5.51	$1g_{9/2}$	0.46	5.431	1g9/2	0.74
		$1f_{5/2}$	0.32	5.732	2d5/2	0.22
14	6.43	$\{$ $\mathbf{2p_{3/2}}$	**0.45**	6.457	2p3/2	1.52
		$\{$ $\mathbf{1f_{5/2}}$	**0.95**	6.520	1f5/2	2.28
		$\{$ $2p_{1/2}$	0.44			
		$\{$ $1f_{5/2}$	1.00			

Table. 2. continued

15	6.68	$2p_{3/2}$	0.66	6.701	2p1/2	1.29
		$2p_{1/2}$	**0.70**			
16	7.34	$2d_{5/2}$	0.17	7.192	na	
		$1g_{9/2}$	0.19	7.401	1f5/2	0.90
17	7.63	**$2p_{3/2}$**	**0.23**	7.643	2p3/2+1f5/2	0.40+0.61
		$1f_{5/2}$	**0.32**			
		$2p_{1/2}$	0.23			
		$1f_{5/2}$	0.34			
18	8.50	$(2p_{3/2})$	(0.44)	8.561	1g9/2	3.32
		$1g_{9/2}$	0.86			
		$(2p_{1/2})$	(0.45)			
		$1g_{9/2}$	0.89			
19	9.08	$(2p_{3/2})$	(0.39)	9.142	2d5/2+1g9/2	0.43+0.71
		$1f_{5/2}$	0.23			
		$(2p_{1/2})$	(0.38)			
		$1f_{5/2}$	0.28			
		$(2d_{5/2})$	(0.26)			
		$(1g_{9/2})$	(0.04)			
20	9.88	$(2p_{3/2})$	(0.46)	9.963	1g9/2	2.55
		$1g_{9/2}$	0.39		(1g9/2+2d5/2)	(1.20,0.47)
		$(2p_{1/2})$	(0.47)			
		$1g_{9/2}$	0.41			
		$2d_{5/2}$	0.24			
		$1g_{9/2}$	0.31			

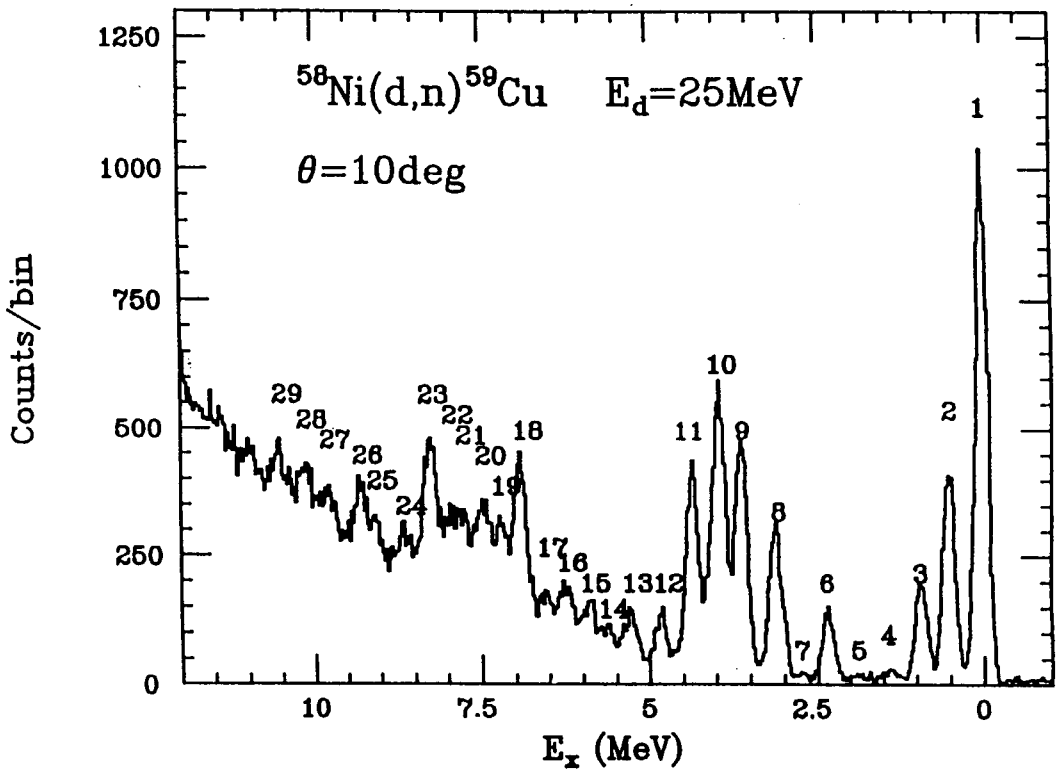

Fig. 1. A typical neutron energy spectrum in the ^{58} Ni (d,n) ^{59} Cu reaction at θ_L=10° .

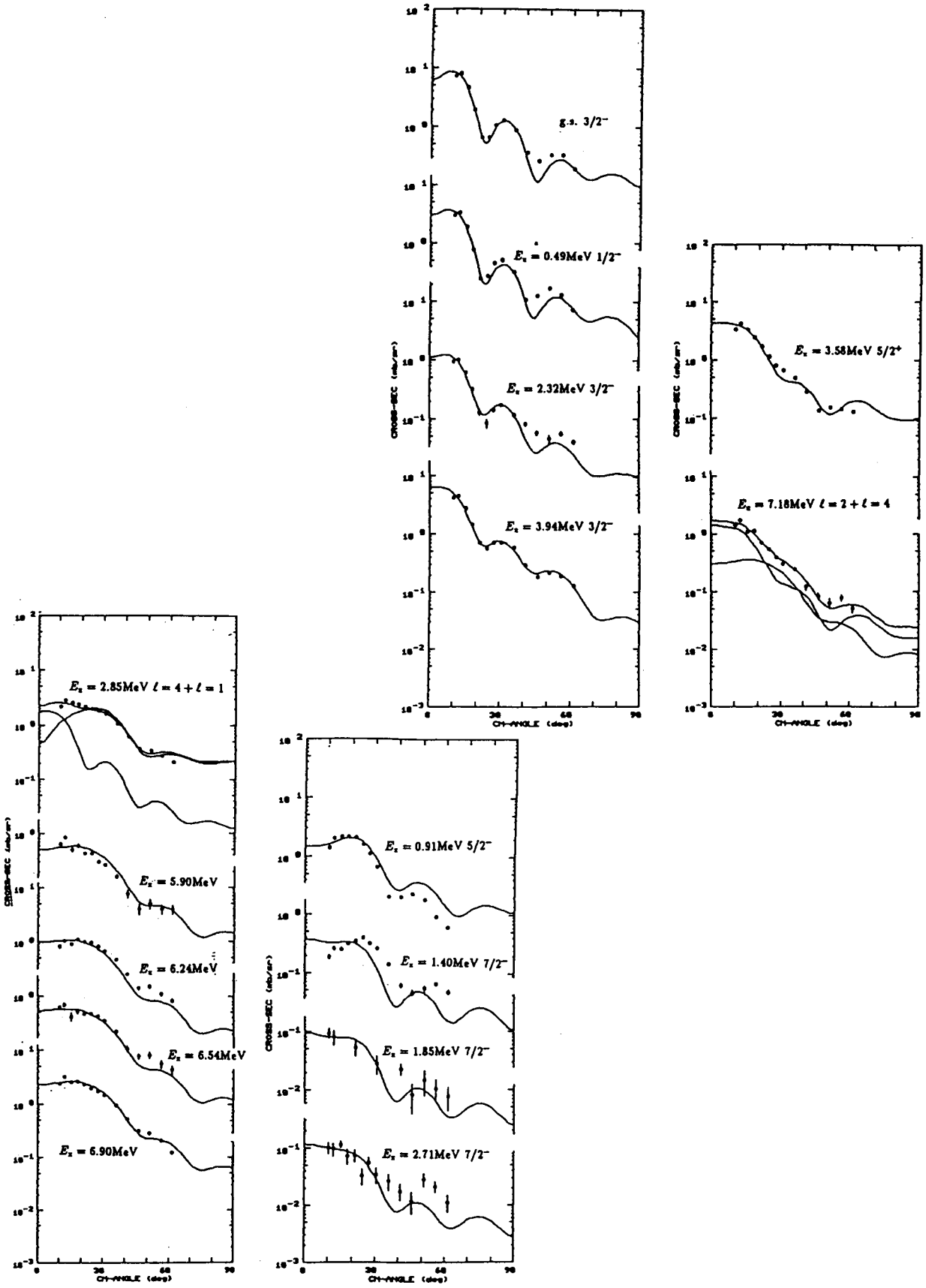

Fig. 2. Typical differential cross sections for the ℓ=1-4 transitions in the ^{58}Ni (d,n) ^{59}Cu reaction. Solid lines are theoretical predictions described in the text.

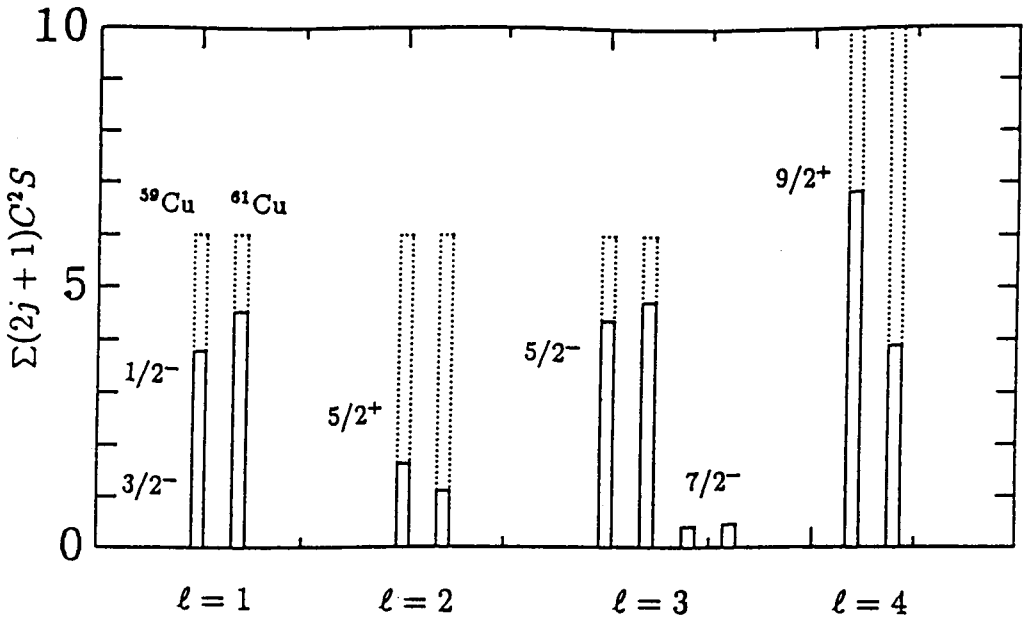

Fig. 3. Summed spectroscopic factors for the e=1-4 transitions in ^{59}Cu and ^{60} Cu.

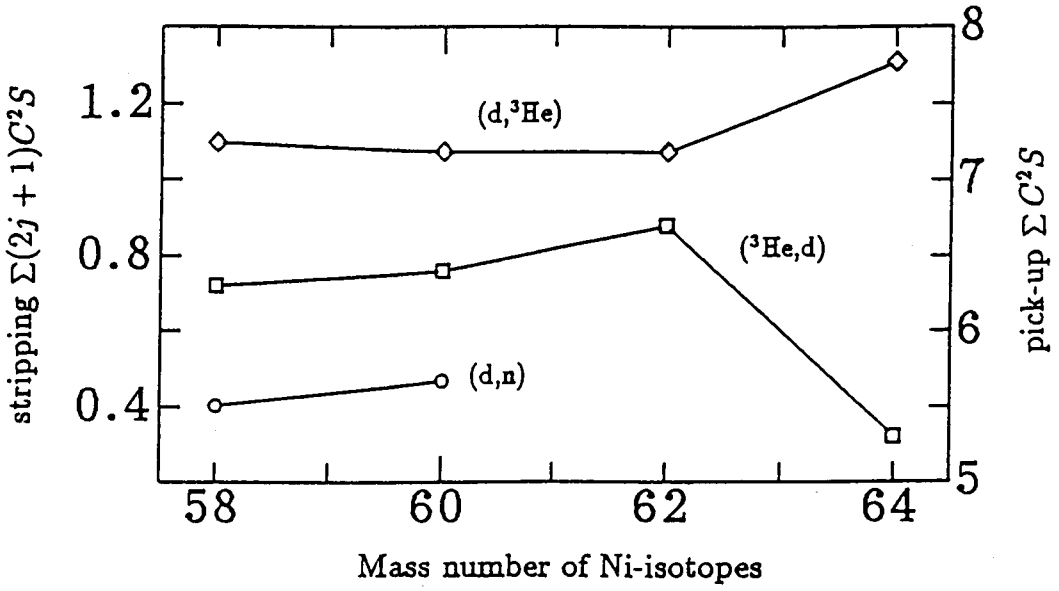

Fig. 4. Mass number dependence of the sum of spectroscopic factors for $1f_{7/2}$ obtained from proton stripping and pick-up reactions on the Ni-isotopes.

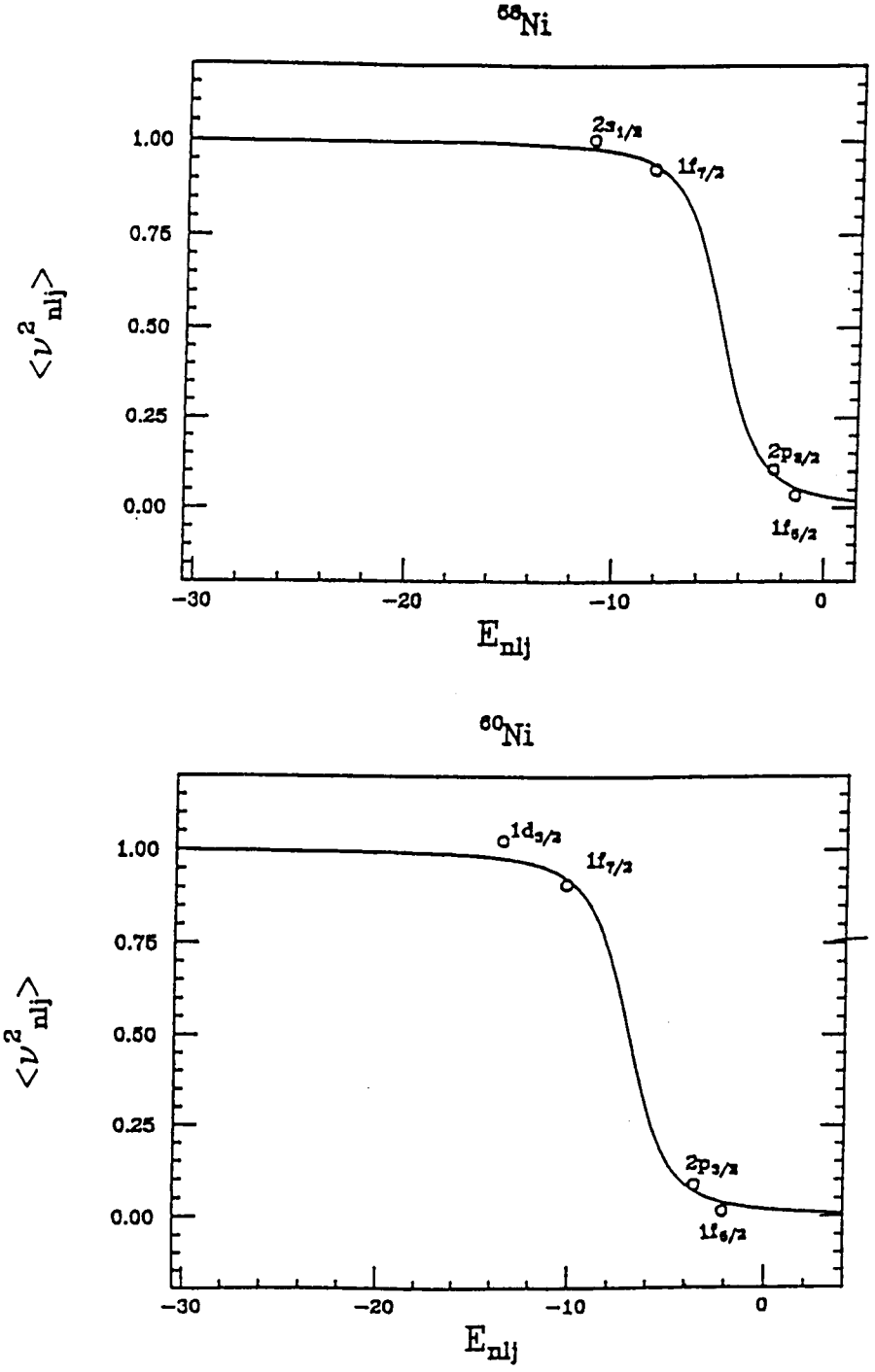

Fig. 5. Distributions of obtained occupation probabilities of proton orbits in ^{58}Ni and ^{60}Ni. Solid lines are fits of the BCS function to the data.